SIMPLIFIED METHOD TO ANALYZE CONTINUOUS RC BEAMS DURING FIRE EXPOSURE

S.F. El-Fitiany and M.A. Youssef *

Biography:

ACI student member **S.F. El-Fitiany** is a Ph.D. candidate at Western University, Canada. Mr. El-Fitiany obtained his MESc from Western University and his BSc from Alexandria University, Egypt. His research interests include behavior of structures during and after exposure to fire and development of performance based fire design approaches.

ACI member **M.A. Youssef** is an associate professor of Civil and Environmental Engineering at Western University. He is an Associate Member of ACI Committee 216 (*Fire Resistance and Fire Protection of Structures*). His research interests include: modeling of reinforced concrete structures, fire resistance of concrete structures, and using shape memory alloys to minimize structural damage during earthquakes.

ABSTRACT

Structural engineers are in need of analytical tools to evaluate the performance of Reinforced Concrete (RC) structures during fire events. Existing numerical methods require extensive knowledge of heat transfer calculations and the finite element method. This paper proposes a rational method to track the fire performance of continuous RC beams during ASTM-E119 standard fire exposure. The proposed method utilizes a simplified sectional analysis approach and is based on separating the effects of thermal deformations and vertical loads. The effective

* Corresponding authors: E-mail: youssef@uwo.ca, Phone: 519-661-2111 Ext. 88661

flexural stiffness and the thermal deformations of the beam are estimated using simple expressions that are developed based on a comprehensive parametric study.

Keywords: Concrete; Elevated temperatures; Sectional analysis; Fire performance, Flexural stiffness, Thermal expansion.

INTRODUCTION

Fire safety is an important design aspect that engineers must consider while designing Reinforced Concrete (RC) structures. Fire initiates by the ignition of combustible materials and spreads horizontally and vertically based on the compartment boundaries[1]. The exposed RC elements are heated and a temperature gradient is generated through them. The developed elevated temperatures cause the element's stiffness to degrade and produce thermal deformations[2, 3]. The only available approach to predict the behavior of a RC element during a fire event is to conduct a nonlinear coupled thermal-stress Finite Element (FE) analysis[4]. The FE method has proven to be a powerful method to predict the behavior of concrete structures during exposure to fire events[4]. Drawbacks of using the FE method including: the need for a comprehensive computer program, the difficulty to comprehend its results and to identify potential modeling errors, and the long running time make it impractical for design engineers. Its complexity becomes obvious in indeterminate structures where different regions of the structure have different heating regimes, cross-section dimensions, reinforcing bars configuration, and axial restrain conditions[5]. A simplified method to estimate the capacities and deformations of statically determinate RC elements during fire exposure was developed and validated by the authors[2, 6, 7]. Although this method is relatively easy to apply as compared to the FE method, it still requires knowledge of heat transfer principles and ability to conduct analysis at elevated temperatures.

In this paper, the fire behavior of statically determinate and indeterminate RC beams is discussed. A practical method for tracking the deflection of indeterminate RC beams during fire exposure is presented and illustrated. The rectangular RC beams tested by Lin et al.[5] are used to validate the proposed method. A number of RC rectangular sections with different cross-section dimensions, reinforcement configuration, material properties, and loading levels are then analyzed during the standard ASTM-E119 fire exposure. Results of the parametric study are used to provide designers with simplified expressions for the effective flexural stiffness and thermal deformations of fire exposed RC beams. These expressions will allow them to easily apply the proposed approach and have a quick idea about the serviceability of RC beams during fire events.

RESEARCH SIGNIFICANCE

Analysis of RC continuous beams for structural fire safety can only be conducted at the research level and requires long computation time. This limitation is due to the complexity of the fire problem and the need for comprehensive FE tools. Fire ratings are currently satisfied using prescriptive methods that include specifying the minimum required cover[8]. Engineers need simplified tools to predict the behavior of RC structures during fire events. These tools are mostly needed by emergency response teams as a quick assessment of the integrity of a fire-damaged structure ensures the safety of their field members. This paper presents such a tool for RC beams.

SECTIONAL ANALYSIS AT ELEVATED TEMPERATURES

Fire temperature drastically decreases concrete and steel mechanical properties and induces thermal and transient strains. Total concrete strain at elevated temperatures (ε) is composed of three terms: unrestrained thermal strain (ε_{th}), instantaneous stress related strain (ε_c), and

transient creep strain (ε_{tr}). Fire performance of RC beams can be predicted by summing these strain components as shown in Eq. (1).

$$\varepsilon = \varepsilon_{th} + \varepsilon_c + \varepsilon_{tr} \quad (1)$$

A sectional analysis approach suitable for the analysis of rectangular RC beams at elevated temperatures was proposed by El-Fitiany and Youssef [2, 6, 7]. Fig. 1a shows the fiber model of a typical RC cross-section. The section is assumed to be exposed to fire from three sides. The approach can be briefly explained by the following main steps:

1. At specific fire duration, a heat transfer analysis is conducted to predict the temperature distribution using the Finite Difference Method (FDM)[1]. The cross-section is then divided into horizontal layers and two average temperatures, T_σ and T_{th} are calculated for each layer. T_σ produces the same average concrete compressive strength for the layer, and thus is suitable for strength calculations. T_{th} represents the algebraic average temperature of the elements within each layer and is suitable for calculating the thermal and transient creep strains as they are temperature dependent[2].

2. The nonlinear thermal strain (ε_{th}) distribution, shown in Fig. 1f, is calculated using T_{th}. The thermal strain of steel bars is calculated based on the concrete temperature at their location. ε_{th} is then converted to an equivalent linear thermal strain ($\overline{\varepsilon_{th}}$), Fig. 1c, by considering self equilibrium of internal thermal forces in concrete and steel layers. The linear distribution is characterized by the unrestrained thermal axial strain, ε_i, and curvature, ψ_i. Fig. 1e shows the differences between the equivalent linear and nonlinear thermal strains, which represent the self induced thermal strains (ε_{st}). These strains are assigned as initial strains for the concrete and steel layers to model the corresponding self-induced thermal stresses at a given point of the fire temperature-time curve. The total strain (ε) can be described as follows:

$$\varepsilon = \overline{\varepsilon_{th}} + \varepsilon_{st} + \varepsilon_c + \varepsilon_{tr} \quad (2)$$

3. The terms ε_{st} , ε_c , and ε_{tr} are lumped into an equivalent mechanical strain ε_{cT} that is used to calculate the corresponding stresses. The constitutive stress-strain relationships for concrete and steel, which are proposed by Youssef and Moftah[3] and are based on T_σ, are adapted. The concrete model implicitly accounts for transient creep as the strain corresponding to the maximum concrete stress is shifted using the transient creep strain given by Terro[9].

4. By considering the equilibrium of the stresses developed in all of the layers, the corresponding moment can be calculated. The behavior of the analyzed cross-section is presented by moment (M)–curvature (ψ) diagram.

The following section presents application of the method to two fire-exposed determinate beams.

STATICALLY DETERMINATE RC BEAMS DURING FIRE

Beams B-123 and B-123a have a cross-section of $305 \times 355\ mm$ [$12 \times 14\ in$] and are fabricated with carbonate aggregate. The compressive strength for concrete, f'_c, is $30\ MPa$ [$4{,}350\ psi$]. The yield strength, f_y, for longitudinal reinforcing bars is $435.8\ MPa$ [$63{,}200\ psi$]. The tensile strength for concrete is neglected[3,10]. The thermal properties proposed by Lie et al.[1] are used for the heat transfer analysis. The constitutive stress-strain relationships for concrete and steel proposed by Youssef and Moftah[3] are used in the analysis of B-123 and B123-a.

Simply supported beam (sagging moments)

The $6.10\ m$ [$1.86\ ft$] simply supported beam (B-123) was tested by Lin et al.[5] and subjected to four-$20\ kN$ [$4.5\ kips$] concentrated loads. Fig. 2a shows the test setup, loading, and beam cross-section. The applied loads were kept constant during exposure to ASTM-E119 standard fire. At

ambient temperature, the applied loads induce an external moment that equals 42% of the beam nominal flexural capacity. A sectional analysis is conducted at different fire durations and the moment (M)–curvature (ψ) diagrams are constructed for each duration. Fig. 2b shows the $M-\psi$ diagrams at ambient temperature and after $30\,min$ of fire exposure. The mid-span deflection is then calculated by integrating the curvature distribution along the beam length. An ABAQUS FE model is also developed[11]. The thermal and stress FE analyses are assumed to be uncoupled. The concrete and steel are modeled using 8-node brick linear elements. Fig. 2c shows a good match between the sectional analysis predictions, ABAQUS FE results, and the experimental data. The sectional analysis has the advantages of ease of application and speed over the FE method.

Cantilever beam (hogging moments)

Experimental and analytical results addressing the fire performance of rectangular beams subjected to hogging (negative) moments is limited in the literature. The behavior of a cantilever beam, B-123a, is analytically studied during exposure to ASTM-E119 fire. As shown in Fig. 2d, the beam supports a uniformly distributed gravity load ($w = 34\,kN/m$) [$25.1\,kips/ft$] and is exposed to fire at three of its surfaces. An ABAQUS uncoupled thermal-stress FE analysis is conducted to predict its behavior. The concrete and steel are modeled using 8-node brick linear elements. The change of the deflection at the end of the cantilever as function of the fire duration is plotted in Fig. 2e. Using the sectional analysis method, the M–ψ diagrams are constructed at different fire durations and the end displacement is then predicted. Fig. 2e shows an acceptable agreement between the sectional analysis and the ABAQUS results. At the beginning, the bottom fibers of the beam, which are located close to the fire temperature, tend to expand relative to the top fibers causing an upward deflection. As fire continues, the stiffness of the beam degrades and

the effect of gravity loads becomes more predominant causing a downward deflection. The difference between the FE method and the sectional analysis results can be due to the use of an average layer temperature and/or the method used to model the tensile reinforcing bars (lumped at one point in the sectional analysis method and represented using the actual circular cross-section area of the bar in the ABAQUS FE model).

MOMENT–CURVATURE RELATIONSHIPS OF FIRE-HEATED RC SECTIONS

Fig. 3 shows schematics for the M–ψ curves for RC sections subjected to sagging and hogging moments at a specific fire duration[4, 7]. The end point on the curve defines the nominal moment capacity (M_n) that corresponds to the curvature capacity of the analyzed cross-section[3]. The secant slope of the M–ψ diagram represents the cross-section's stiffness at a specific moment (M_{app}) or at a specific load level (λ), $\lambda = M_{app}/M'_n$ and M'_n is the nominal flexural capacity at ambient temperature.

For a specific fire duration, the effect of thermal strain on the M–ψ relationship is not governed by the load level. It represents the free thermal expansion of the unloaded concrete element and results in shifting the M–ψ diagram by a value ψ_i. The shift can be predicted by calculating the nonlinear thermal strain distribution and converting it to an equivalent linear distribution as discussed earlier in this paper. The $M-\psi$ diagram includes the effects of material degradation, transient creep strain (ε_{tr}), and self induced thermal strain (ε_{st}). The total curvature (ψ) is the sum of the unrestrained thermal curvature (ψ_i) and the mechanical curvature (ψ_{cT}) and can be expressed in terms of the effective stiffness (EI_{eff}) as follows.

$$\psi = \psi_i + M_{app}/EI_{eff} \quad (3)$$

As shown in Fig. 3, heating RC beams from the bottom face and the two sides cause the bottom

concrete fibers to thermally expand more than the top concrete fibers and results in ψ_i. The acting moment induces a mechanical curvature (ψ_{cT}), which is either added to or deducted from ψ_i. As shown in Fig. 3a, a positive (sagging) moment induces a curvature that adds to the initial curvature. For negative (hogging) moments, compression stresses are applied on the bottom fibers. Curvature caused by these stresses opposes the initial curvature, Fig. 3b. Such a moment-curvature diagram is similar to that of a prestressed concrete beam section. While the initial curvature in such a beam is caused by prestressing, it results from the thermal expansion in a fire-exposed beam. The moment required to shift the behavior from sagging to hogging is a function of the fire duration that is proportional to the value of the initial curvature and the section properties that affects flexural deformations. The effect of fire duration and different section properties are discussed in details in the parametric study conducted at the end of this paper.

STATICALLY INDETERMINATE RC BEAMS DURING FIRE

Indeterminacy restrains thermal deformations and induces secondary moments. The following sections propose and validate a method to track the behavior of statically indeterminate beams during fire exposure.

Proposed method for continuous RC beams

The main assumptions of the proposed method are:

1) The effect of heat transfer along the beam longitudinal axis is neglected, i.e. two-dimensional heat transfer for the beam cross-section is conducted using the FDM.

2) The effect of concrete cracking on the heat transfer calculations is neglected.

3) The tensile resistance of concrete is assumed equal to zero.

4) Plane sections remain plane during fire exposure. This assumption has been validated using available experimental results up to a fire temperature of 1100 ℃ [2012 °F][2].

5) The thermal expansion is not affected by the load level.

6) The beam can be divided into elements, each with a constant stiffness EI_{eff}.

7) Transient $creep\ strains$ are calculated using Terro's model[9] and are implicitly accounted for by using the stress-strain relationship proposed by Youssef and Moftah[3].

Fig. 4a shows a schematic for a two span RC continuous beam subjected to fire from its bottom face and two sides. The beam is divided into five segments (S1, S2, S3, S2, and S1) based on the reinforcement configuration. The ambient temperature (primary) BMD is shown in Fig. 4b. The behavior of this beam at specific fire duration (t) is affected by the values of the degraded stiffness (EI) and the thermal deformations. To capture this behavior, the following steps are proposed.

I) Evaluating the degraded flexural stiffness

A sectional analysis is conducted for the beam sections and the $M-\psi$ diagram is constructed for each segment at the given fire duration (t), Fig. 4c. The effective flexural stiffness (EI_{eff}) for each segment is then evaluated as the secant slope of the $M-\psi$ diagram at the applied ambient moment level. As a conservative simplification, a constant value of EI_{eff} is assigned to each segment based on its maximum flexural moment[12], Fig. 4d. Revised values for M_1, M_2, and M_3 are to be calculated based on the degraded EI_{eff} values.

II) Evaluating the restrain effect on thermal deformations

The unrestrained thermal curvature ψ_i is the curvature value at zero moment. Fig. 4d shows the distribution of ψ_i along the beam length during fire exposure. The continuity of the beam prevents this distribution from forming. Assuming that the middle support is removed, the

curvature distribution, shown in Fig. 4d, can be obtained by applying two imaginary concentrated thermal moments (M_{th}) at the ends of each segment, Fig. 4e. Because of the continuity of the beam (the middle support in this example), the applied thermal curvatures cannot form. Secondary moments are developed in the beam redistributing these curvatures. These secondary moments can be evaluated by analyzing the indeterminate beam under the effect of the thermal moments (M_{th}), shown in Fig. 4e. Such analysis leads to defining the reaction at the middle support that can be used to calculate the moment diagram, Fig. 4f. The final moment acting on the beam equals the summation of the primary and secondary moments. This method is similar to the one used to account for the effect of restraint in continuous prestressed concrete beams.

The mentioned steps are repeated by recalculating the values for EI_{eff} that corresponds to the final moment distribution. These values are used to recalculate the primary and secondary moments. Iterations are performed until convergence is reached.

Validation of the proposed methodology

Lin et al.[5] have experimentally investigated the effect of continuity on the behavior of RC beams during fire exposure. Fig. 5a shows a schematic of beam B-124 and Fig. 5b shows its reinforcement. The beam dimensions are the same as B-123. The beam was exposed to a 3.5 hrs of ASTM-E119 standard fire over a length of 5.486 m [18 ft], Fig. 5a, while supporting four equally spaced concentrated loads ($P3$) and two end loads ($P1$) and ($P2$). $P3$ was kept constant at 50.2 kN [11.27 kips] during the fire test. Prior to the fire test, $P1$ and $P2$ were equal to about 59.0 kN [13.26 kips]. They were adjusted during the fire test such that the deflections at points A and B are kept constant. The beam own weight is 2.57 kN/m [0.175 kips/ft]. The beam supports an additional load at the center span of 0.53 kN/m [0.036 kips/ft], which represents the weight of the

furnace cover. At ambient temperature, the applied loads induce flexural negative and positive moments of about 43% of the beam nominal flexural capacity. Fig. 5c shows the moment diagram as compared to the nominal moment capacity. The beam was fabricated using carbonate concrete having a compressive strength of $29.7\ MPa$ [$4310\ psi$]. The yield strength of the reinforcing bars was $435.8\ MPa$ [$63{,}200\ psi$]. The mid-span deflection of the intermediate span and the variable loads $P2$ and $P3$ were monitored during the fire test. These values are predicted using the proposed method in the following section.

Modeling and analysis of B-124

The RC continuous beam is modeled using SAP2000[13] software as a series of frame elements. For simplicity, the beam is considered symmetric in terms of loading and material properties. To account for concrete cracking at ambient temperature, the M–ψ diagrams are constructed for both positive and negative moment sections and used to define (EI_{eff}) for the three cross-sections shown in Fig. 5b. The vertical loads are applied on the beam and the corresponding deflections are shown in Fig. 5d. The calculated mid-span deflection at ambient temperature is 0.015 m [0.57 in]. The upward deflection at the beam ends is 0.003 m [0.11 in]. During fire exposure, the behavior of beam B-124 is studied by super-positioning the thermal and load effects.

Unrestrained thermal curvature

A heat transfer analysis is conducted for B-124 using the FDM and the thermal properties given by Lie et al.[1]. The obtained temperature distributions, at different fire durations, are used to evaluate the equivalent linear thermal strain distributions for both the maximum negative and maximum positive moment sections. Fig. 6 shows the variation of the unrestrained thermal curvature (ψ_i) at different fire durations up to $3.5\ hrs$.

Flexural stiffness of during fire exposure

The beam is divided based on the applied load level and fire exposure conditions to seven segments as shown in Fig. 5e. Sectional analysis is conducted for each segment at different fire durations. Using the obtained moment-curvature diagrams, the secant modulus of elasticity, (EI_{eff}), is estimated. Fig. 7a shows the degradation of EI_{eff} for the heated positive moment section at load level (λ) equals to 43% and 28% up to 3.5 hr of ASTM-E119 fire exposure. The reduction in EI_{eff} for the fire exposed negative moment section is shown in Fig. 7b. The temperature of steel bars is considered uniform along the beam length because of the high thermal conductivity of steel material[1].

Applying the proposed approach on B-124

The performance of B-124 after 1 hr of ASTM-E119 standard fire exposure is predicted by applying the following steps:

1- To simulate the support conditions during the fire test, the vertical displacement calculated at ambient condition, i.e. U3 = 0.0027 m [0.106 in], is applied as an induced displacement at the cantilever ends.

2- From Fig. 7, the reduced (effective) flexural stiffnesses, (EI_{eff}), are $3.10 \times 10^{12}\ N.mm^2$ and $3.53 \times 10^{12}\ N.mm^2$ for the positive moment segments and $2.86 \times 10^{12}\ N.mm^2$ and $15.10 \times 10^{12}\ N.mm^2$ for the negative moment segments. [$1\ N.mm^2 = 1/2870\ Ib.in^2$]

3- An arrangement of concentrated moments is applied on the beam to represent the unrestrained thermal curvatures. Fig. 5e. The corresponding curvature values, Fig. 6, are $8.65 \times 10^{-6}\ \frac{1}{mm}$ and $1.48 \times 10^{-5}\ \frac{1}{mm}$ for the positive and negative moment sections, respectively. ($\frac{1}{mm} = 25.4\ \frac{1}{in}$).

The mid-span deflection and the vertical reactions at the outer supports are recorded, Fig. 5f. These reactions are used to calculate the secondary moment that is induced during fire exposure,

Fig. 8a. The total BMD is the summation of the primary moment, i.e. at ambient temperature, and the secondary moment as shown in Fig. 8b.

4- The final moment distribution changes the applied load levels (λ) along the beam length, Fig. 8b. The new λ values are used to recalculate EI_{eff} in the second iteration. This procedure is repeated till convergence for EI_{eff} is achieved. Fig. 8b indicates that the reduced negative flexural capacity for the main span, i.e. $M_n = -63.83\ kN.m\ [-47.08\ kips.ft]$, governs the overall capacity of the beam. Since the location of the zero moment is shifted from its original position at ambient temperature, the behavior of a section within the main span subjected to negative moment is studied in the subsequent analysis cycle. The convergence of B-124 is achieved after three analysis iterations.

The previous steps are repeated each $15\ min$ up to $3.5\ hrs$. Fig. 9 shows the variation of mid-span deflection during the fire test. B-124 should theoretically fail after 160 min of ASTM-E119 fire exposure if the moment redistribution is neglected. By accounting for the secondary moments generated during fire exposure, the prediction of the mid-span deflection is significantly improved and matches the measured deflection data experimentally with a maximum error of 22% at 105 min. The difference between the analytical and test results can be due to the inaccurate predictions of λ during the analysis and the complexity of test conditions. The effect of beam continuity and moment redistribution on the cantilever loads $P1$ and $P2$ is shown in Fig. 10. The proposed approach has acceptable predicted the variation of $P1$ and $P2$ during fire exposure with an error in the order of 15%.

EVALUATION OF THERMAL AND EFFECTIVE STIFFNESS PARAMETERS

In this section, the effects of different geometric and material factors on the unrestrained thermal

curvature (ψ_i) and on the effective flexural stiffness (EI_{eff}) are discussed using a comprehensive parametric study. The study aims at providing structural engineers with simple expressions to evaluate these parameters without the need for heat transfer and sectional analysis calculations.

Table 1 summarizes the properties of the analyzed beams. All the beams have rectangular cross-section and are subjected to ASTM-E119 standard fire exposure from three sides as shown in Fig. 11. The considered parameters are width (b), height (h), concrete compressive strength (f'_c), flexural moment at ambient temperature ($\lambda = 15\% - 60\%$), number of tensile steel layers ($n = 1, 2$), aggregate type (Agg) (siliceous, carbonate), compression reinforcement ratio ($\rho' = 0.06\% - 0.65\%$), and tensile reinforcement ratio ($\rho = 0.5\% - 2.5\%$). Each of the shown sections is analyzed twice, considering its performance in positive and negative bending. The standard reinforcement layout, shown Fig. 11, is assumed in this study. The parametric study is limited to siliceous and carbonate concretes with compressive strength (f'_c) ranging between 20 and 50 MPa [1 MPa = 145.04 psi]. The fire duration (t) ranges from 0.0 to 2.5 hr.

Unrestrained thermal curvature

A heat transfer analysis is conducted for each of the assumed sections and the nonlinear thermal distribution is converted to a uniform thermal distribution. The unrestrained thermal curvature ψ_i is estimated at each time step up to 2.5 hr. Fig. 12 shows the variation of ψ_i for the studied sections considering both positive and negative bending. As fire temperature/duration increases, larger thermal strains develop and the initial curvature ψ_i is increased. Assuming the same ρ and ρ', ψ_i for sections subjected to negative moments is found to be higher than ψ_i for sections subjected to positive moments. This can be explained by the fact that both sections have almost the same thermal expansion at their bottom layers. However, the top thermal strain will be lower

for sections subjected to negative moments as the increased area of top steel bars that have relatively low temperatures limit the expansion of the top layers. The effect of tensile reinforcement ratios (ρ) and compressive concrete strengths (f'_c) on ψ_i is found to be negligible.

The effect of the cross-section dimensions, b and h, is shown in Figs. 12a and 12b. Increasing the section height (h), or decreasing the section width (b), decreases ψ_i. Deep sections spread the thermal expansion over longer length. This results in decreasing ψ_i. ψ_i is significantly increased for wide sections. This is due to the low thermal conductivity of concrete, which results in a substantial thermal expansion difference between the lower and top concrete masses.

Distributing the tensile steel bars on two layers ($n = 2$) instead of one layer ($n = 1$) has a minor effect on ψ_i for sections subjected to negative moment. For sections subjected to positive moments, the effect of n is clear because of the lower temperature in the second row. Increasing the compression reinforcement ratio ρ' reduces ψ_i for sections subjected to positive moments. The effect of compression reinforcement in the case of negative moment is minimal as it is exposed to high temperatures, which reduce its effectiveness in controlling ψ_i.

Concrete with carbonate aggregate is found to have less thermal expansion than concrete with siliceous aggregate[1, 3]. The effect of the aggregate type on the curvature is minor for the case of positive moment as the thermal expansion of the lower concrete is highly dependent on the expansion of the bottom steel reinforcement. The thermal expansion of the lower concrete mass is more predominant in case of negative moments as its expansion is not controlled by substantial amount of steel bars.

Proposed expressions for the unrestrained thermal curvature ψ_i

The values obtained from the parametric study for ψ_i are analyzed using a multiple regression

analysis technique[14]. This has resulted in equations (4) and (5) that can be used to predict the unrestrained thermal curvature ψ_i for rectangular RC sections subjected to ASTM-E119 fire exposure up to $2.5\ hr$. Eq. (4) is for sections subjected to positive (sagging) moments and Eq. (5) is for sections subjected to negative moments. The predictions of the proposed equations are shown in Fig. 12.

$$\psi_i = 10^{-7} \times [\, -0.1994 - 1.023 \times 10^{-2}\, b\, .\, t^5$$
$$+(\, 4.072 \times 10^{-2}\, b + \, 8.683)\ t^4$$
$$-(38.884 + 2.025 \times 10^{-2}\, b)\, t^3$$
$$+(46.997 - 8.670 \times 10^{-2}\, b)\, t^2$$
$$+(68.490 - 0.07108\, h + 0.103\, b - 5.968\, \rho'\,)\, t$$
$$+(11.131\, n\, .\ Agg - 23.381\, Agg - 8.897\, n)\, t\ ] \qquad (4)$$

$$\psi_i = 10^{-7} \times [\, -0.9604 - 6.698\, t^4$$
$$+(62.166 - 3.430 \times 10^{-2}\, h)\, t^3$$
$$+(-214.634 + 0.185\, h)\, t^2 + (348.066$$
$$-0.372\, h + 0.09388\, b - 13.252\, Agg\,)\, t\ ] \qquad (5)$$

Where,

ψ_i is the unrestrained thermal curvature at fire duration $t \geq 0.25\ hrs$

t is the ASTM-E119 fire duration in hrs

b is the cross-section width in mm [$1\ mm = \ 1/25.4\ \ in$]

h is the cross-section height in mm [$1\ mm = \ 1/25.4\ \ in$]

ρ' percentage of compression reinforcement relative to $(b \times d)$

d is the effective depth of tensile reinforcement in mm [$1\ mm = \ 1/25.4\ \ in$]

n is the number of tensile reinforcement layers

Agg is a factor to account for the aggregate type (0.0 for siliceous concrete and 1.0 for carbonate concrete)

Fig. 13 shows the relationship between the analytical predictions, using the sectional analysis, and the values obtained by applying the proposed expressions.

Effective flexural stiffness

Using the obtained moment-curvature relationships, the secant slope (EI_{eff}) is evaluated at four load levels, $\lambda = 15\%, 30\%, 45\%, and\ 60\%$, for different fire durations. As a sample of the results, Fig. 14 shows the effect of tensile reinforcement ratio, ρ, and duration of fire exposure on EI_{eff} for a number of the studied rectangular RC beams. Similar to ambient temperature, EI_{eff} of RC beams depends on the tensile reinforcement ratio (ρ)[12]. While for positive bending, fire severely affects the yielding strength of the tensile reinforcing bars, it degrades the compressive concrete strength in case of negative bending. Both the loading level (λ) and the aggregate type (Agg) have a minor effect on the stiffness degradation.

Proposed expressions for the effective flexural stiffness EI_{eff}

The effective flexural stiffness at ambient temperature can be estimated using Eq. (6) that is was developed based on an analytical study[12] and was included in ACI 318-08[15].

$$\frac{EI_{eff}}{E_c I_g} = (0.10 + 0.25\,\rho)\left(1.2 - 0.2\,\frac{b}{d}\right) \leq 0.5 \qquad (6)$$

Where,

EI_{eff} is the effective flexural stiffness at ambient temperature (i.e. $t = 0.0\ hrs$)

E_c is the ambient secant modulus for concrete and can be evaluated in MPa as $4500\sqrt{f'_c}$ [$1\ MPa = 145.04\ psi$] [8]

f'_c concrete compressive strength in MPa [$1\ MPa\ =\ 145.04\ psi$]

I_g gross sectional second moment of inertia

b is the cross-section width in mm [$1\ mm\ =\ 1/25.4\ in$]

d is the effective depth of tensile reinforcement in mm [$1\ mm\ =\ 1/25.4\ in$]

ρ percentage of tensile reinforcement relative to $(b \times d)$

During ASTM-E119 fire exposure, Eqs. (7) and (8) are proposed to predict the degradation of the effective flexural stiffness EI_{eff} for sections subjected to positive and negative moments, respectively. These equations are developed based on a multiple regression analysis of the parametric study results, Fig. 15. The proposed equations are shown in Fig. 14. An upper limit for these equations is considered to be given by Eq. (7).

For sections subjected to positive moments

$$\frac{EI_{eff}}{E_c I_g} = 2.032 \times 10^{-2}$$

$$-(0.180 + 1.408\,\rho)\,{}^{1}\!/_{t^2} \times 10^{-2}$$

$$+(\,5.897 +\ 10.806\,\rho) \times \frac{1}{t} \times 10^{-2}$$

$$+(2.590\,\lambda + 0.651\,Agg)t^2 \times 10^{-2}$$

$$-(12.676\,\lambda + 0.375\,Agg)\,t \times 10^{-2}\ \ \leq \text{Eq. (6)} \qquad (7)$$

For sections subjected to negative moments

$$\frac{EI_{eff}}{EI_g} = -0.210 \times 10^{-2} - (1.329 + 0.506\,\rho$$

$$-1.762\,\lambda - 0.14\,\rho')\frac{1}{t^2} \times 10^{-2} +(\,5.414 + 4.2\,\rho'$$

$$-2.948\,\lambda + 4.747\,\rho)\,\frac{1}{t} \times 10^{-2} \qquad \leq \text{Eq. (6)} \qquad (8)$$

Where,

t is the ASTM-E119 fire duration in hrs ($t \geq 0.25\ hr$)

Agg is a factor to account for the aggregate type (0.0 for siliceous concrete and 1.0 for carbonate concrete)

λ is the flexural level at ambient temperature

Practical application of the proposed method

The proposed method described in this paper can be used by designers to check the fire ratings of simple and continuous RC beams subjected to standard ASTM-E119 fire exposure. The steps of the proposed method can be summarized as follows:

- analyze the beam at ambient temperature and calculate the primary BMD. The beam is then divided into a number of segments based on the calculated BMD and fire exposure conditions.
- evaluate the degraded flexural stiffness (EI_{eff}) at specific fire duration using Eqs. (7) and (8).

A constant value of EI_{eff} is assigned to each segment of the beam based on its maximum flexural moment.

- estimate the unrestrained thermal curvature ψ_i for each beam segment using Eqs. (4) and (5).

A set of concentrated moments are applied to the fire exposed region of the beam to induce the unrestrained thermal curvature distribution during fire exposure.

- analyze the beam and estimate the secondary moment distribution as well as the deflected shape. The secondary moments are added to the primary moments to predict the total moment distribution. Revised values for EI_{eff} are assigned to each beam segment based on the predicted total moment distribution. An iterative procedure should be done till convergence is achieved.
- The previous steps are repeated at different fire durations to predict the fire performance of the considered beam.

SUMMARY AND CONCLUSIONS

A sectional analysis methodology was proposed by the authors in previous publications[2,7]. The application of this methodology for statically determinate beams is presented in this paper and extended to predict the fire performance of statically indeterminate RC beams. A practical approach based on superimposing the effects of thermal expansion and material degradation is introduced. The nonlinear thermal expansion is converted to an equivalent uniform thermal distribution, which can be represented by the unrestrained thermal axial strain ε_i and curvature ψ_i. The degradation effect in material strength is considered by accounting for the reduction in the effective flexural strength (EI_{eff}). The RC continuous beam tested by Lin et al.[5] is used to validate the proposed terminology. The mid-span deflections as well as the outer supports` reactions are predicted up to 3.5 hrs of standard ASTM-E119 fire exposure. A good agreement is found between the experimental data and the results of the proposed methodology.

A comprehensive parametric study is conducted in the second part of the paper to investigate the effect of different material, geometric, and loading factors on the unrestrained thermal curvature (ψ_i) and the effective flexural strength (EI_{eff}). For simplicity, the parametric study is limited to rectangular RC beams subjected to $2.5\,hr$ ASTM-E119 standard fire exposure and typical reinforcement configurations. Based on the results of the parametric study, a number of expressions are proposed to predict ψ_i and EI_{eff} for sections subjected to both sagging (positive) and hogging (negative) moments. Designers can apply the proposed methodology using these expressions to conduct a quick assessment for the structural fire safety of RC continuous beams.

ACKNOWLEDGMENTS

This research was funded by the Natural Sciences and Engineering Research Council of Canada.

REFERENCES

1. Lie, T.T., ed., "Structural Fire Protection," ASCE Manuals and Reports on Engineering Practice, no. 78, New York, NY, 1992, 241 pp.
2. El-Fitiany, S., Youssef, M.A., "Assessing the flexural and axial behaviour of reinforced concrete members at elevated temperatures using sectional analysis", Fire Safety Journal, vol. 44, no. 5, 2009, pp. 691-703.
3. Youssef, M.A. and Moftah, M., "General stress-strain relationship for concrete at elevated temperatures," Engineering Structures, vol. 29, no. 10, 2007, pp. 2618-2634.
4. Kodur, V.K.R., and Dwaikat, M., "Performance-based fire safety design of reinforced concrete beams," Journal of Fire Protection Engineering, vol. 17, no. 4, 2007, pp. 293-320.
5. Lin, T.D., Gustaferro, A.H., and Abrams, M.S., "Fire Endurance of Continuous Reinforced Concrete Beam", Portland Cement Association, Bulletin RD072.01B, Skokie, 1981.
6. El-Fitiany S.F. and Youssef M.A., “A Simplified Sectional Analysis Approach for RC Elements during Fire Events”, 6th International Conference on Structures in Fire, Michigan State University in East Lansing, MI, 2010, pp. 239-246.
7. El-Fitiany, S.F., and Youssef, M.A., “Stress Block Parameters for Reinforced Concrete Beams During Fire Events,” Innovations in Fire Design of Concrete Structures, ACI SP-279, 2011, pp. 1-39.
8. Cement Association of Canada, “Concrete design handbook, CAN/CSA A23.3-04," 3rd Ed., Ottawa, 2006.
9. Terro, M.J., "Numerical modeling of the behavior of concrete structures in fire", ACI Structural Journal, vol. 95, no. 2, 1998, pp. 183-193.
10. Youssef, M.A., EL Fitiany, S.F., and Elfeki, M.A., "Flexural Behavior of Protected Concrete Slabs after Fire Exposure", Designing Concrete Structures for Fire Safety, ACI SP-255,

2008, pp. 47-74.

11. ABAQUS theory and user manuals version 6.9. USA: ABAQUS Inc..
12. Khuntia, M., and Ghosh, S. K., “Flexural Stiffness of Reinforced Concrete Columns and Beams: Analytical Approach,” ACI Structural Journal, vol. 101, no. 3, May-June, 2004, pp. 351-363.
13. Wilson EL. SAP2000 analysis reference manual. Berkeley, California: Computers and Structures Inc.; 2002.
14. Ronald J. Wonnacott. & Wonnacott, Thomas H., (fourth edition), “Introductory statistics”, New York: John Wiley & Sons, 1985.
15. ACI Committee 318,“Building Code Requirements for Structural Concrete (ACI 318-08) and Commentary,” American Concrete Institute, Farmington Hills, MI, 2005, 465 pp.

TABLES AND FIGURES

List of Tables

List of Figures

Table 1–Parametric study cases

Beam #	b (mm) [in]	h (mm) [in]	f'_c (MPa) [psi]	n	ρ' % (A_g)	ρ % (A_g)
B1	300 [11.8]	500 [19.7]	30 [4351]	1	0.13	0.5
B2						1.0
B3				2		1.5
B4						2.5
B5	300 [11.8]	700 [27.6]		1	0.10	0.5
B6				2		1.0
B7						1.5
B8						2.5
B9	400 [15.7]	700 [27.6]		2	0.07	1.0
B10						2.5
B11	500 [19.7]	700 [27.6]		2	0.06	1.0
B12						2.5
B13	300 [11.8]	300 [11.8]		1	0.22	1.5
D1	300 [11.8]	500 [19.7]	20 [2901]	1	0.13	0.5
D2						1.0
D3				2		1.5
D4						2.5
D5	300 [11.8]	700 [27.6]	40 [5802]	1	0.10	0.5
D6				2		1.0
D7						1.5
D8						2.5
D9	400 [15.7]	700 [27.6]	50 [7252]	2	0.07	1.0
D10						2.5
D11	500 [19.7]	700 [27.6]	50 [7252]	2	0.06	1.0
D12						2.5
I1 *	300 [11.8]	500 [19.7]	30 [4351]	1	0.13	1.0
I2 *				2	0.13	2.5
I4	300 [11.8]	700 [27.6]	40 [5802]	2	0.25	1.0
I5					0.45	
I6					0.65	
I7 *	300 [11.8]	700 [27.6]	30 [5802]	2	0.10	1.5
I8 *	300 [11.8]	700 [27.6]	40 [5802]	2	0.10	0.5
I9 *					0.10	1.5
I10	400 [15.7]	700 [27.6]	50 [7252]	2	0.15	2.5
F1	300 [11.8]	500 [19.7]	30 [4351]	2	0.13	1.5
F2	300 [11.8]	500 [19.7]	30 [4351]	2	0.13	1.5
F3	300 [11.8]	700 [27.6]	30 [4351]	2	0.10	2.5

* carbonate aggregate

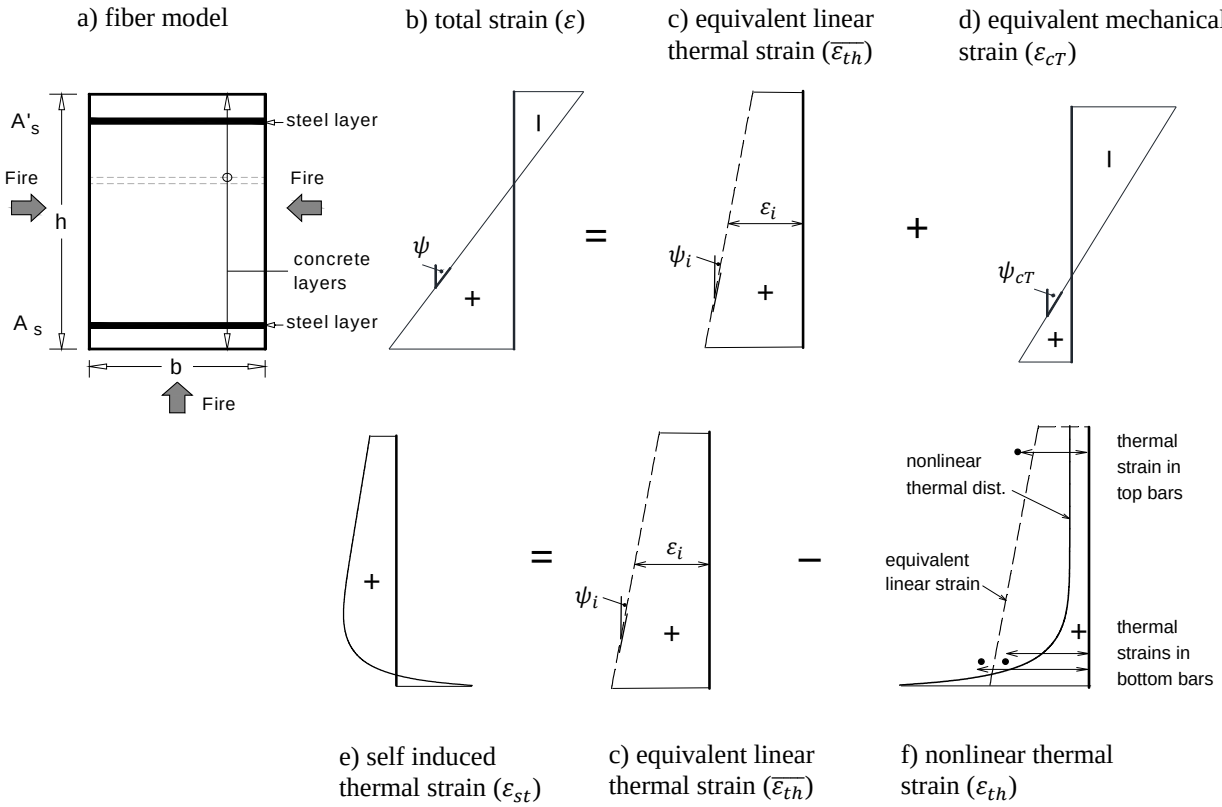

Fig. 1-Modified sectional analysis approach for RC sections exposed to fire

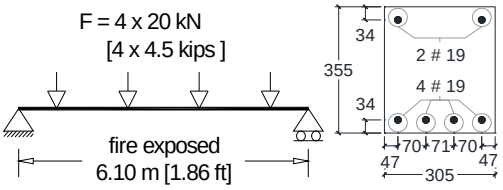

a) beam loading (B-123)

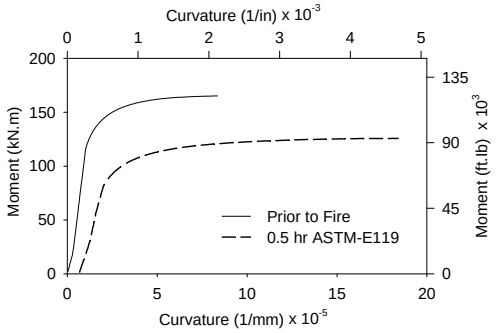

b) M – ψ diagram (B-123)

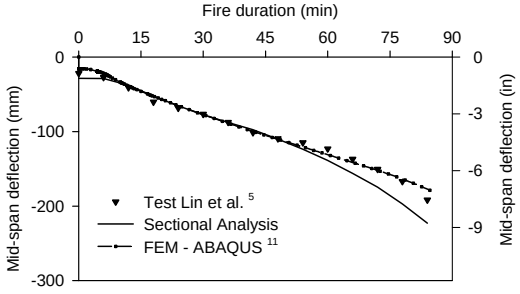

c) mid-span deflection (B-123)

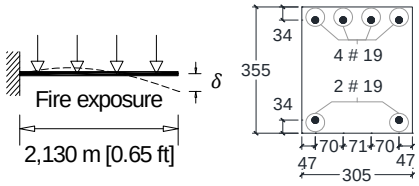

d) beam loading (B-123a)

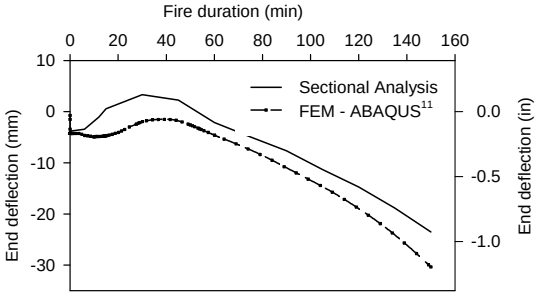

e) cantilever deflection (B-123a)

Fig. 2-Validation beams (B-123) and (B-123a)

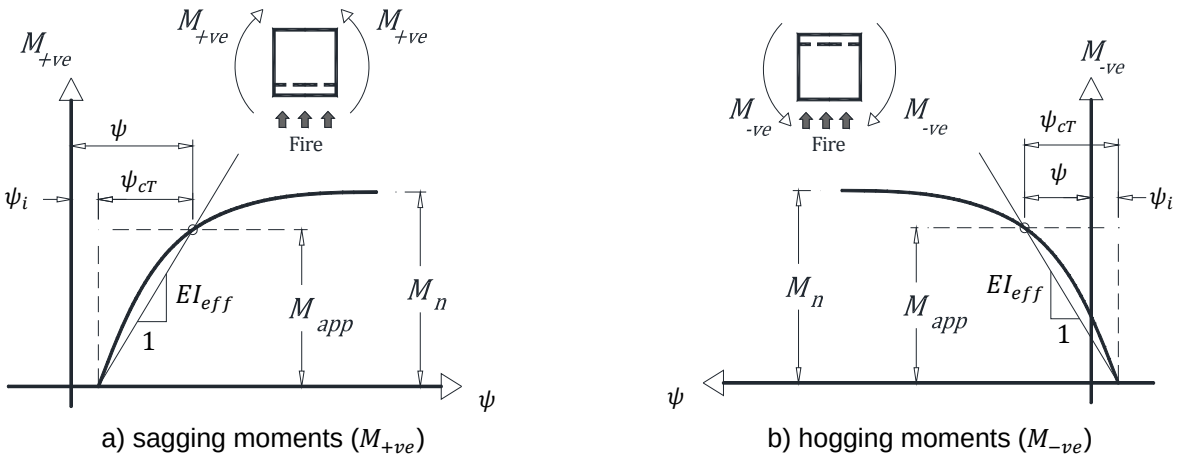

a) sagging moments (M_{+ve}) b) hogging moments (M_{-ve})

Fig. 3-(M)–(ψ) diagrams for RC beams during fire

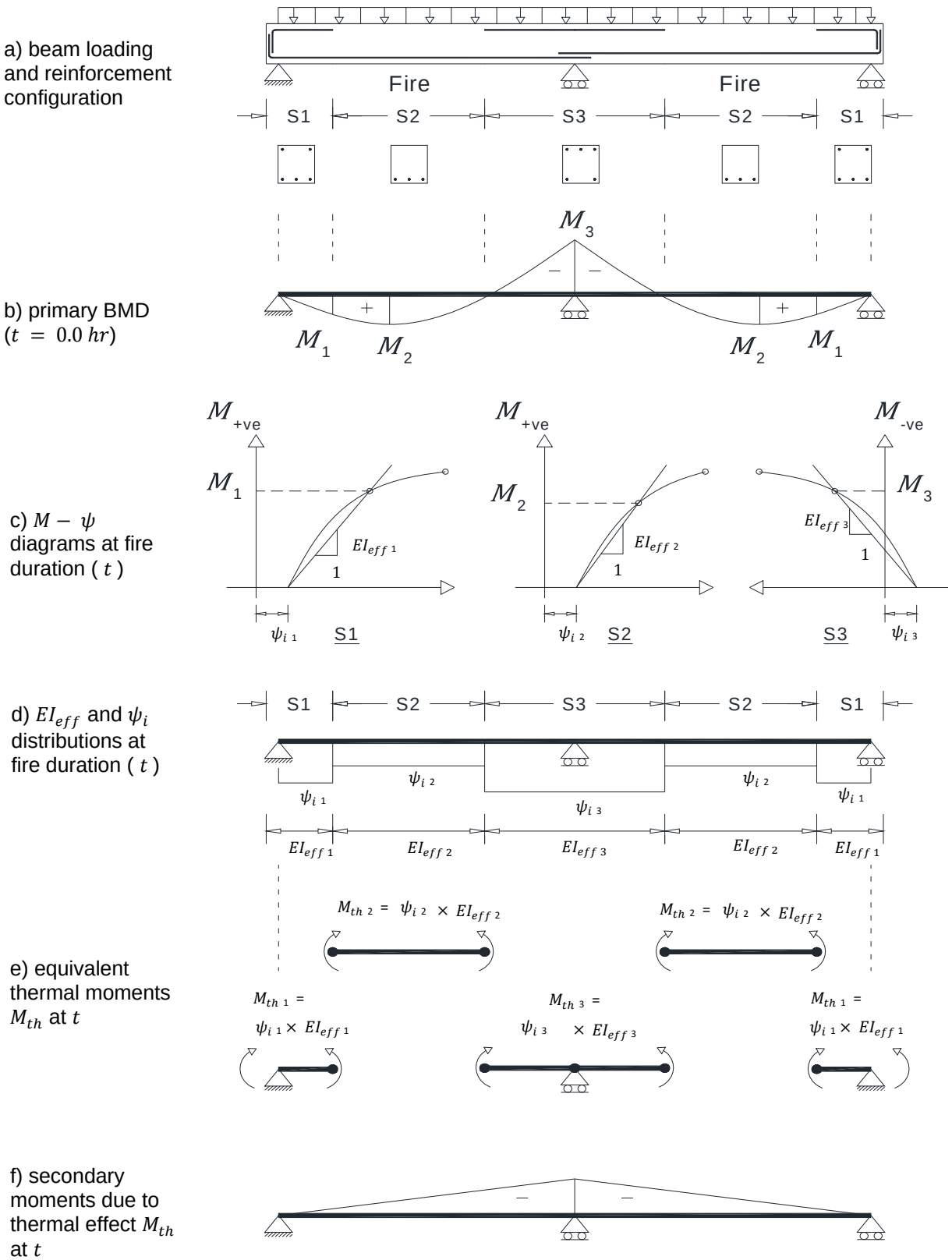

Fig. 4-Analysis steps for a two-span continuous RC beam during fire

a) beam loading

(Dimensions in m [$1\ m\ =\ 3.28\ ft$])

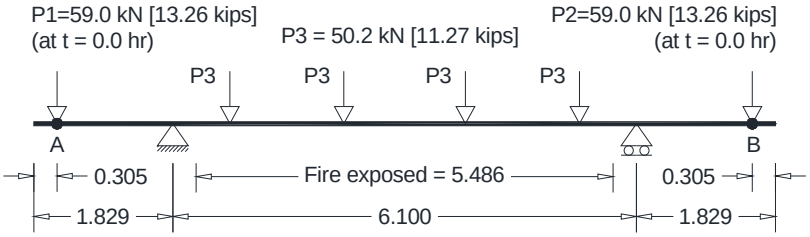

b) reinforcement configuration

(Dimensions in m [$1\ m\ =\ 3.28\ ft$])

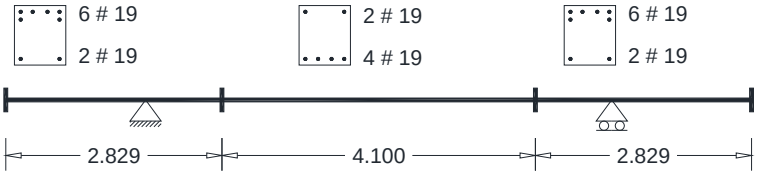

c) Primary BMD ($t\ =\ 0.0\ hr$)

(Moments in $kN.m$ [$1\ kN.m\ =\ 737.56\ Ib.ft$])

(Stiffnesses in $N.mm^2$)
[$1\ N.mm^2\ =\ 1/2870\ Ib.in^2$]

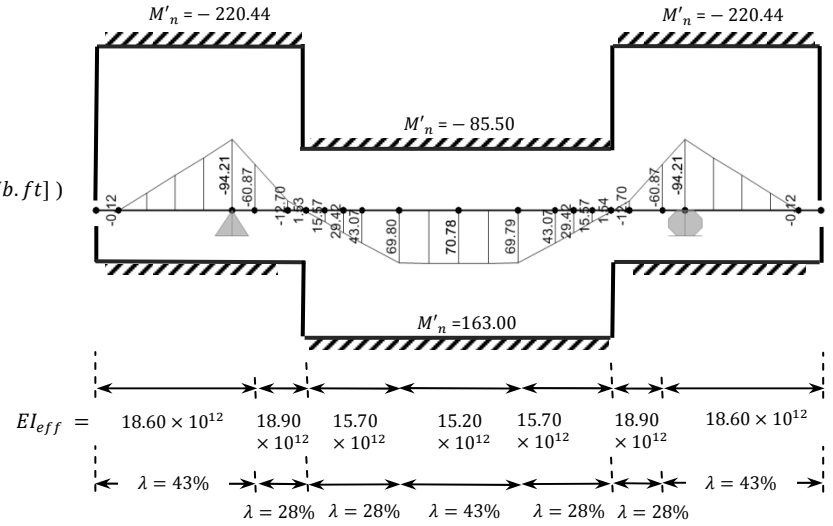

d) beam deflection ($t\ =\ 0.0\ hr$)

(Dimensions in m [$1\ m\ =\ 3.28\ ft$])

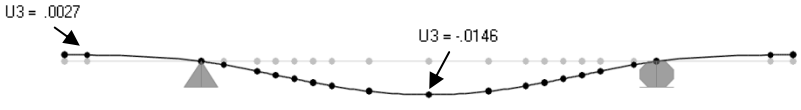

e) fire loading ($t\ =\ 1.0\ hr$)

(Dimensions in m [$1\ m\ =\ 3.28\ ft$])

(Stiffnesses in $N.mm^2$)
[$1\ N.mm^2\ =\ 1/2870\ Ib.in^2$]

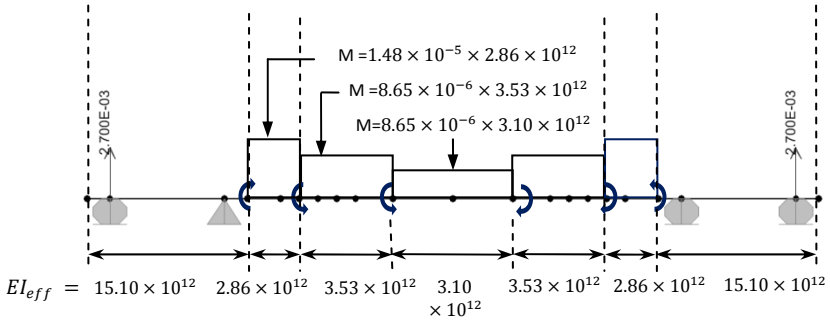

f) beam deflection and reactions ($t\ =\ 1.0\ hr$)

(Dimensions in m [$1\ m\ =\ 3.28\ ft$])

(Reactions in kN [$1\ kN\ =\ 224.81\ Ib$])

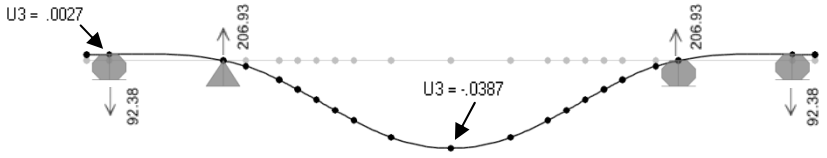

Fig. 5-Validation beam B-124

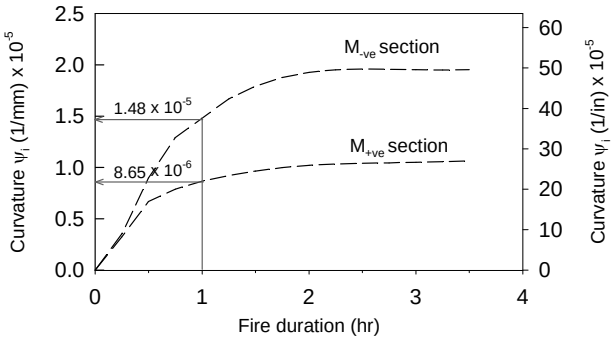

Fig. 6-Unrestrained thermal curvature ψ_i for B-124

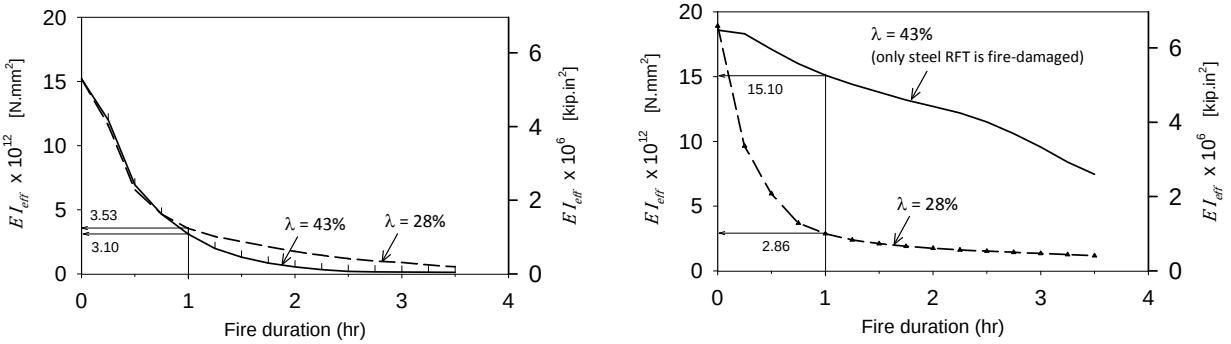

a) M_{+ve} section

b) M_{-ve} section

Fig. 7-Effective stiffness of B-124 during fire test

a) Secondary BMD ($t = 1.0\ hr$)

(Moments in $kN.m$ [$1\ kN.m = 737.56\ lb.ft$])

b) Total BMD ($t = 1.0\ hr$)

(Moments in $kN.m$ [$1\ kN.m = 737.56\ lb.ft$])

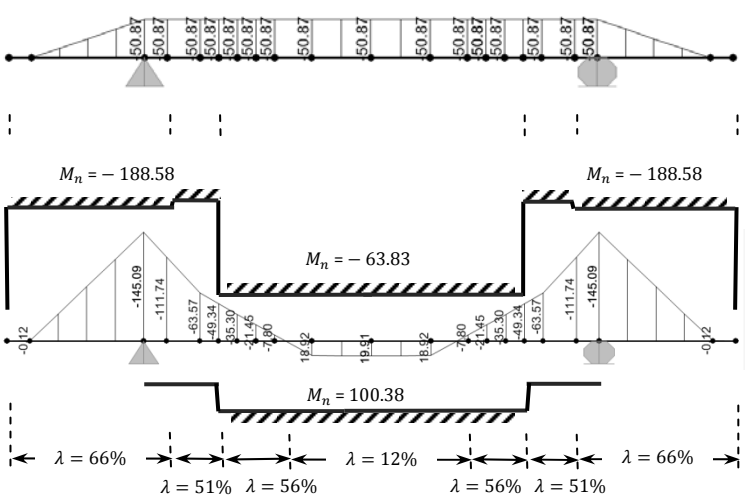

Fig. 8-Moment redistribution of B-124 after $1.0\ hr$ ASTM-E119 fire exposure

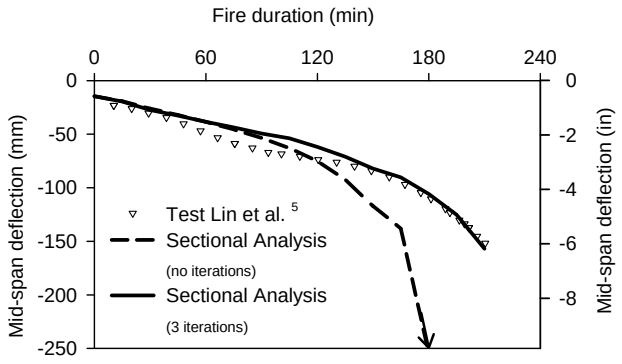

Fig. 9-Mid-span deflection of B-124

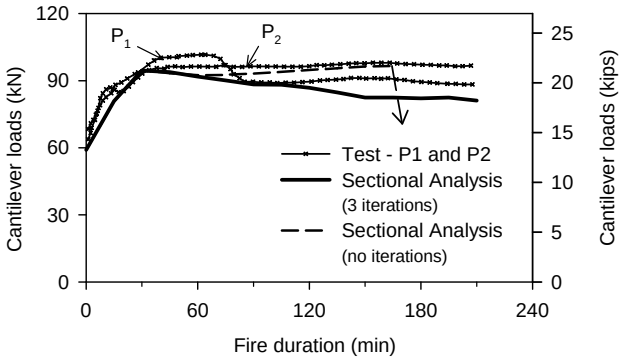

Fig. 10-Outer span loads of B-124

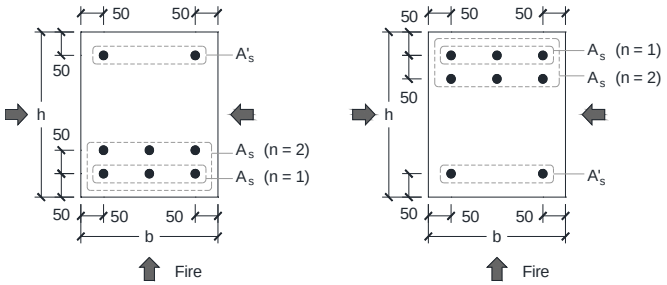

a) sagging moments (M_{+ve})

b) hogging moments (M_{-ve})

Fig. 11-Typical cross-sections for the parametric study beams

(Dimensions in mm [1 mm = 1/25.4 in])

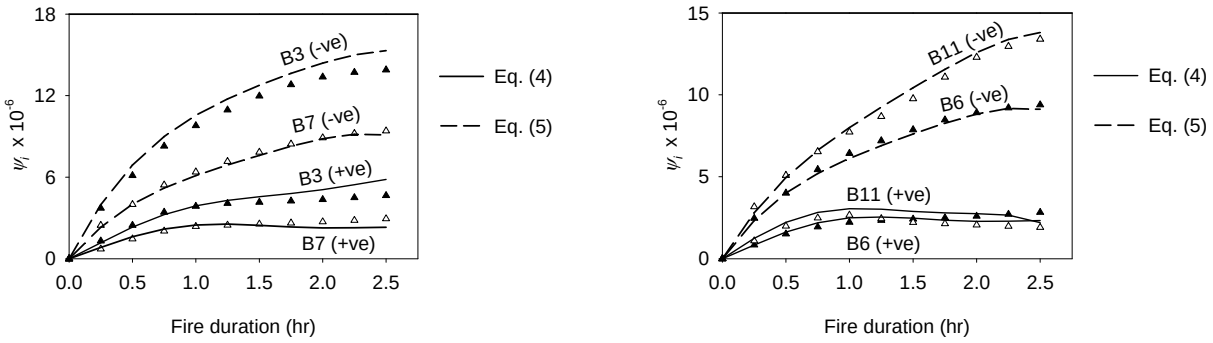

a) effect of section height h

b) effect of section width b

Fig. 12- Effect of section dimensions (b, h) on ψ_i
(Curvature in $1/mm$ [$1/mm = 25.4 \times 1/in$])

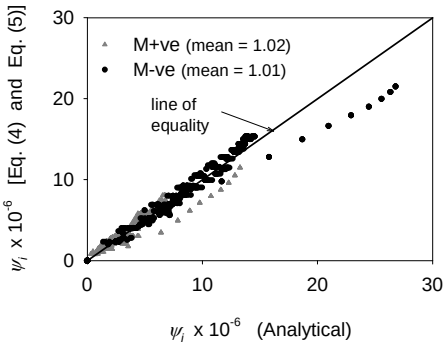

Fig. 13- Regression analysis of ψ_i results
(Curvature in $1/mm$ [$1/mm = 25.4 \times 1/in$])

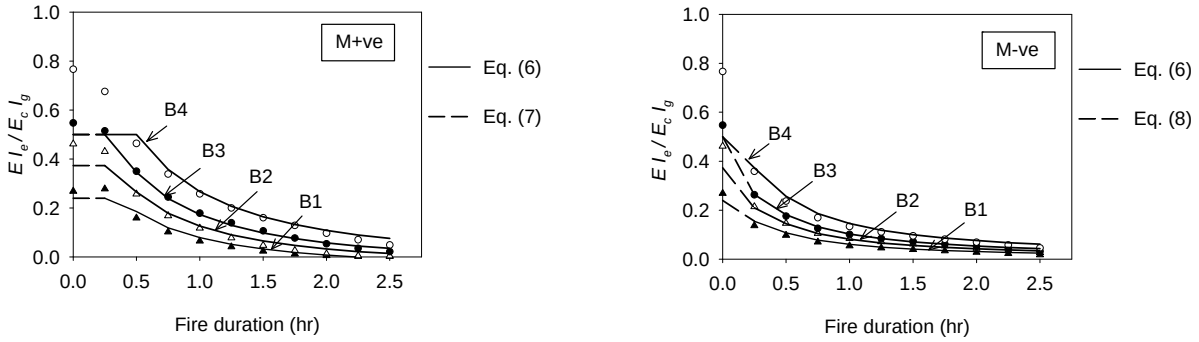

Fig. 14- Effect of tensile reinforcement ratio (ρ) on EI_{eff}

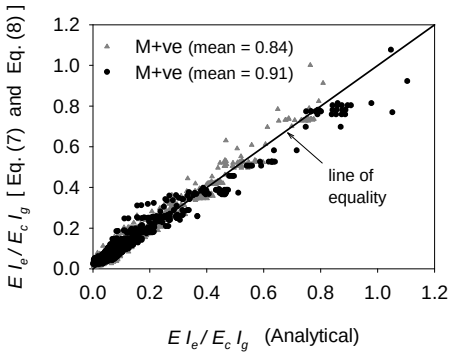

Fig. 15- Regression analysis of EI_{eff}